Unravelling a direct role for polysaccharide β-strands in the higher order structure of physical hydrogels

Unravelling a direct role for polysaccharide *β*-strands in the higher order structure of physical hydrogels

Anja Rüther,[a] Aurelien Forget,[b, c, d] Anjan Roy,[e] Carolina Carballo,[e] Rina K. Dukor,[e] Laurence A. Nafie,[e, f] Christian Johannessen,[g] V. Prasad Shastri,*[c, d] and Steffen Lüdeke*[a]

Abstract: The mechanical properties of agarose-derived hydrogels depend on the scaffolding of the polysaccharide network. To identify and to quantify such higher-order structure, we applied Raman optical activity (ROA), a spectroscopic technique that is highly sensitive toward carbohydrates, on native agarose and chemically modified agarose for the first time in the gel phase. By spectral global fitting, we isolated features that change as a function of backbone carboxylation (28, 40, 50, 60, 80 and 93%) from others that remain unchanged. We assigned these spectral features through comparison to ROA spectra calculated for different oligomer models. We found a 60:40% ratio of double and single stranded α-helix in the highly rigid hydrogel of native agarose, while the considerably softer hydrogels made from carboxylated agarose use a scaffold of unpaired β-strands.

Hydrogels, water swollen cross-linked polymer networks,[1] have found extensive applications in consumer products[2], pharmaceuticals,[1, 3] regenerative medicine,[2, 4] and microfluidics devices.[5] The network formation in hydrogels involves covalent, ionic or physical crosslinks between polymer chains.[1] The nature of the crosslinks can impact many important properties of the gel such as stiffness, porosity and rheology. Hydrogels formed from agarose, a polysaccharide derived from red algae composed of D-galactose and 3,6-anhydro-L-galactopyranose repeat units, undergo thermally reversible gelation through physical crosslinking that involves the aggregation of α-helices.[6] We recently showed that the introduction of carboxylic acid groups along the agarose backbone (carboxylated agarose (CA), Figure 1) promotes the evolution of a β-sheet structure, which leads to the disruption of helical interactions and a different organization and ultrastructure of the gels.[7] As a consequence, the gels are softer and have a lower gelation temperature in comparison to those formed from native agarose (NA).[7] However, similar effects on hydrogel stiffness can also be achieved through the physical blending of NA with highly carboxylated agarose (CA93).[8] Thus, deciphering the true nature of the physical crosslinks in hydrogels formed from polysaccharides that possess both α-helical and β-strand conformation could provide valuable insights for tailoring their mechanical properties and structure. To date, the methods to determine polysaccharide structure are largely borrowed from those used in protein and peptide structure analysis; these include X-ray crystallography, nuclear magnetic resonance (NMR) and circular dichroism (CD) spectroscopy. These methods sample a biomolecule's secondary or tertiary structure that is present in the crystalline or in the solution state. However, for the understanding of the mechanisms that drive the assembly network of polysaccharide strands in a hydrogel it is necessary to monitor the higher-order structure directly in the gel phase. While small-angle x-ray scattering data on agarose gels has been interpreted to result from the presence of α-helix bundles in the gel state,[9] until now, direct evidence on the presence and interplay of this and other polysaccharide species in a hydrogel environment and information on their relative proportion have not been available.

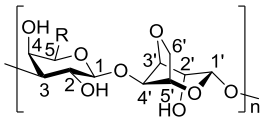

Figure 1. Repeating unit of agarose-derived polysaccharides with R = CH_2OH for NA and R = COOH for CA.

Raman optical activity (ROA), the chiroptical equivalent to Raman spectroscopy, has proven to be highly sensitive toward the conformational and higher-order structure of various biological molecules[10] including carbohydrates.[11] It provides characteristic vibrational spectra from the small difference in Stokes scattering of right minus left circularly polarized light, which arises if an irradiating photon interacts with a chiral sample.[12] One of the virtues of ROA is that the observed spectral patterns can be directly correlated with molecular structure through quantum chemical calculations,[13] which has also been demonstrated for various carbohydrates.[14] Besides other marker bands that arise in a polysaccharide but are absent in the monomeric building blocks,[15] particularly C–O stretch

[a] Dr. A. Rüther, Dr. S. Lüdeke
Institute of Pharmaceutical Sciences
University of Freiburg
Albertstrasse 25, 79104 Freiburg (Germany)
Fax: (+49) 761-203-6351
E-mail: steffen.luedeke@pharmazie.uni-freiburg.de
[b] Dr. A. Forget
Future Industries Institute, University of South Australia, Mawson Lakes (Australia)
[c] Dr. A. Forget, Prof. Dr. V. P. Shastri
Institute for Macromolecular Chemistry
University of Freiburg
Stefan-Meier-Str. 31, 79104 Freiburg (Germany)
Fax: +49 (0)761 203-5016
E-mail: prasad.shastri@gmail.com
[d] Dr. A. Forget, Prof. Dr. V. P. Shastri
BIOSS – Centre for Biological Signalling Studies, University of Freiburg (Germany)
[e] Dr. A. Roy, C. Carballo, Dr. R. K. Dukor, Prof. Dr. L. A. Nafie
BioTools, Inc., Jupiter (USA)
[f] Prof. Dr. L. A. Nafie
Department of Chemistry, Syracuse University, Syracuse (USA)
[g] Prof. Dr. C. Johannessen
Department of Chemistry, University of Antwerp, (Belgium)

Supporting information for this article is given via a link at the end of the document.((Please delete this text if not appropriate))

vibrations involving the glycosidic oxygen have been associated with secondary structure.[16] In this study, we elucidated the higher order structure of polysaccharide chains by analyzing gel phase ROA spectra of hydrogels of NA and CA (28, 40, 50, 60, 80, and 93% carboxylation).

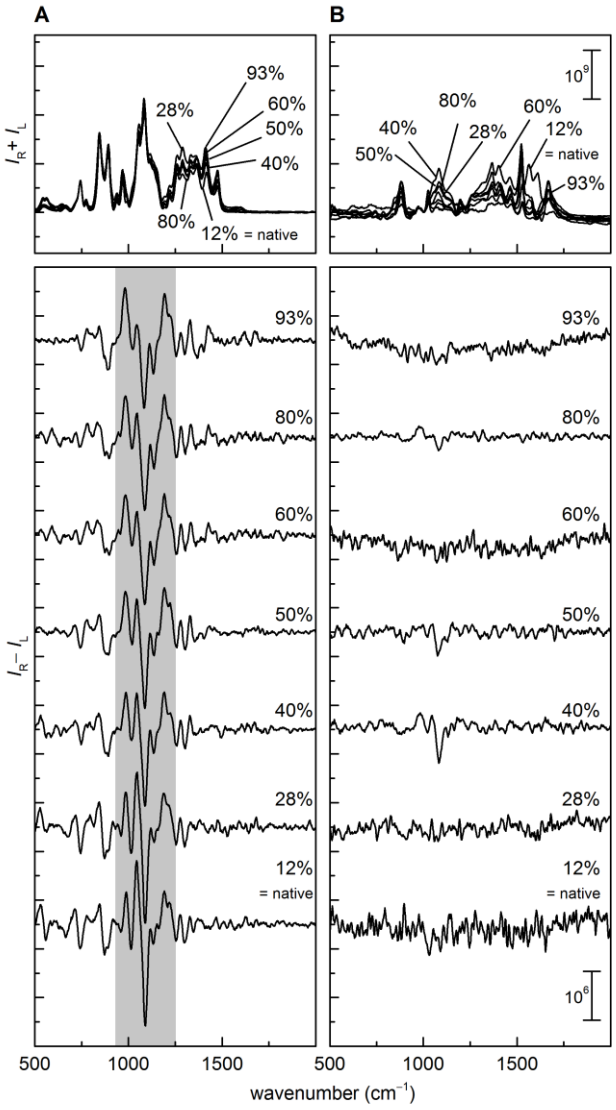

Figure 2. A) Parental Raman spectra (circular intensity sum, $I_R + I_L$, superimposed, see Figure S2 for a detailed representation) and ROA spectra (circular intensity difference, $I_R - I_L$, stacked) of NA and CA with different degrees of modification of the galactose unit at C6. ROA bands in the C–O stretch are highlighted in gray. B) Raman and ROA spectra of hydrolyzed NA and CAs. Depending on the degree of polysaccharide breakdown, spectral features associated with secondary structure are significantly reduced in the oligosaccharide spectra. The Raman spectra are normalized in respect to Raman intensities of NA and hydrolyzed NA. The ROA spectra are normalized with the corresponding scaling factors.

CA was prepared as described previously by oxidation of NA with (2,2,6,6-tetramethylpiperidin-1-yl)oxyl (TEMPO).[7] The polysaccharide hydrogels of NA and CA (2% w/v) show characteristic Raman and ROA spectra (Figure 2A) comprising spectral features that are not present in the calculated or observed spectra of monomeric D-galactose[11b, 14e] or 3,6-anhydro-L-galactopyranose.[11a, 14b] The large polymer signals possibly have their origin in delocalized phonon-like vibrations.[17] In contrary, solution state spectra of NA or CA oligomers obtained from acidic hydrolysis (0.5 M hydrochloric acid, Figure S1), which are devoid of higher-order structure and long-range Raman and ROA effects, show considerably weaker overall intensities (Figure 2B).[18] In the ROA, spectral differences between hydrogels of NA, which may already carry up to 12% modification,[6c, 19] and of CA are most obvious in the C–O stretch region between 1000 and 1100 cm^{-1} and below 900 cm^{-1} (Figure 2A).

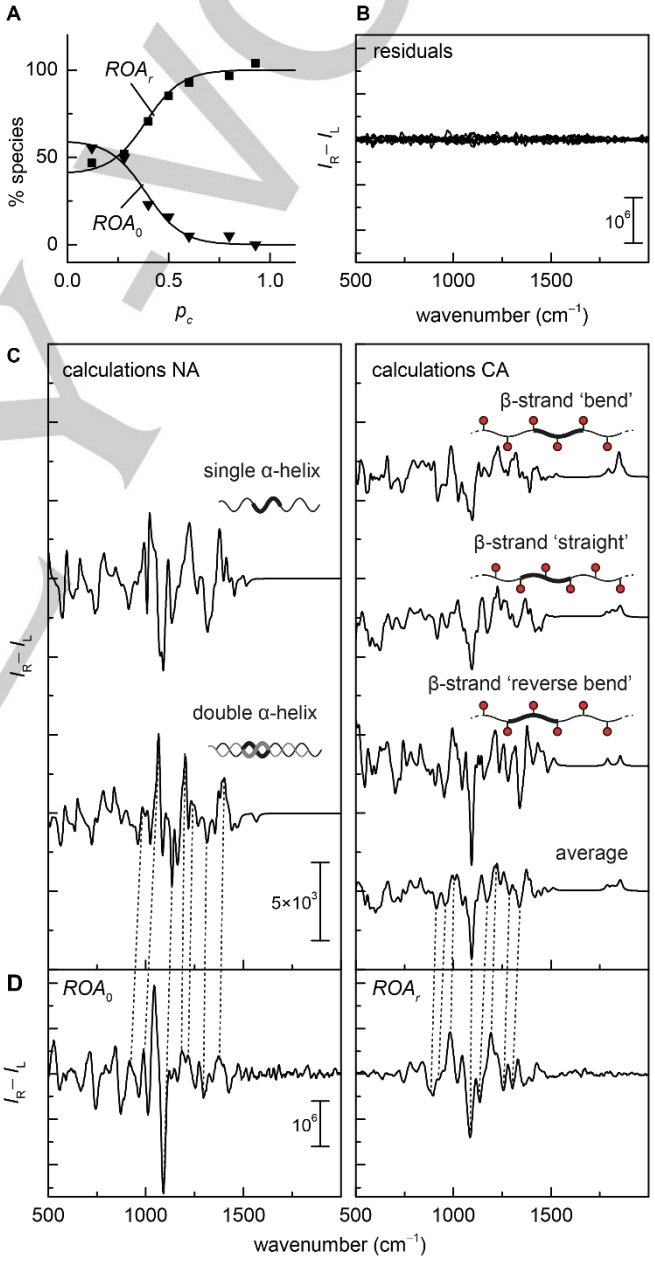

Figure 3. A) Proportion of spectral species that is depleted (ROA_0) and the one that increases as a response to carboxylation (ROA_r) in each spectrum. The progression of the values is well described by a logistic function using k =

19.0 and r_{max} = 0.6, obtained from MLS global fitting. B) Residuals from global fitting. C) Calculated ROA spectra (CPCM/B3LYP/6-31G**//CPCM/B3LYP/rDPS level) of the trimer models of NA and CA (Figure 4). The spectra of β-strand 'bend' and 'straight' are the average spectra for all sub-conformers, weighted according to the cluster analysis of the MD calculation. D) Pure spectra for ROA_0 and ROA_r. Dotted lines connect corresponding bands in the calculated and in the experimental spectra. The assignments were confirmed by the analysis of the corresponding circular intensity differential (CID) spectra (Figure S7).

A hydrogel composed of partially carboxylated agarose should contain at least three conformational species: double α-helix and single stranded α-helical conformation, which are present in NA,[6] and the β-strand conformation that forms upon carboxylation.[7-8] Singular value decomposition (SVD) of the ROA data only delivered two spectral species that are different from noise (Figure S3). This indicates that two out of a number of different conformational species whose relative proportion depends on the degree of carboxylation are distinguishable by ROA.

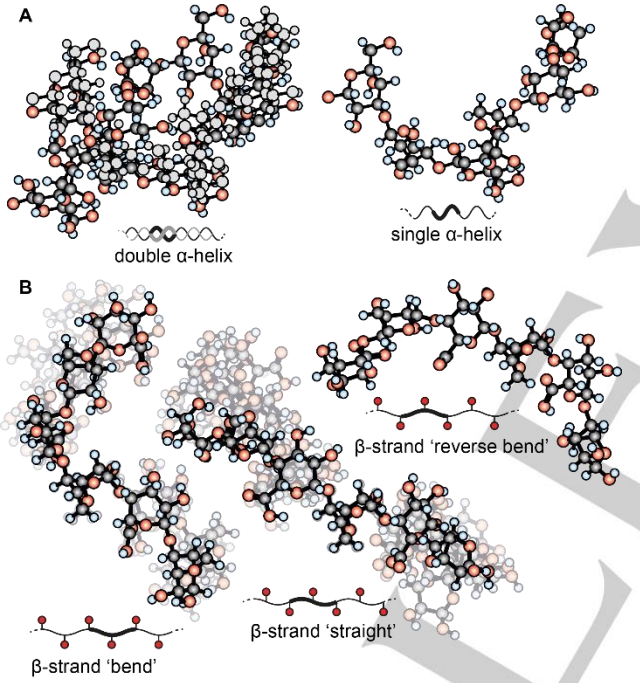

Figure 4. 3D geometry models of trimers underlying the ROA calculations. A) NA double and single α-helix according to 1AGA.[6b] B) The cluster analysis of the MD data delivers three conformer families for CA trimers: β-strand 'straight' (five members) and β-strand 'bend' (four members) and 'reverse bend'. Lower-abundance family members are shaded. The three conformations are interpreted as segments of the polysaccharide structure (structures correspond to heavy lines in the cartoons). Fusion of the segments would result in a chain with zigzag secondary structure (thin lines).

While the ROA spectra change considerably going from 28 through 40 and 50 to 60% carboxylation, the differences between the NA and 28% spectra and also between the 60, 80, and 93% spectra are less pronounced, thereby forming two groups of similar appearance (Figure 2A). This is in agreement with a sigmoidal degree-of-perturbation/response relationship. Major changes in higher-order structure may only take effect when a critical proportion of carboxylation is reached, and, as there is only a limited number of positions that can be carboxylated, the initially exponential evolution of new structure will converge against a specific value of maximum response (r_{max}). Such a cooperative effect is well described by the logistic function:

$$r(p_c) = \frac{r_{max}}{1 + e^{-k \cdot p_c \cdot r_{max}} \left(\frac{r_{max}}{r_0} - 1\right)} \qquad (1)$$

Here, p_c is the proportion of carboxylated galactose units, $r(p_c)$ is the carboxylation-induced response, k is a proportionality constant and r_0 is the value of r for p_c = 0, which is chosen to be close to zero. The carboxylation-dependent ROA spectra can be interpreted as the linear combination of the spectral contributions from the two ROA-sensitive species that are concomitant with $r(p_c)$. We used equation (1) for matrix least squares (MLS) global fitting, a method that incorporates the information of a full-range spectrum in the fitting process.[20] The analysis delivered a sharp transition (inflection at p_c = 0.4) and an r_{max} of 0.6. This means that NA contains 60% of a species that is represented by a spectrum ROA_0, and 40% of a second species represented by ROA_r (Figure 3D, see Supporting Information for details). With increasing degree of carboxylation, contributions from ROA_r increase, while ROA_0 disappears (Figure 3A), therefore the CA 93% spectrum is virtually identical to ROA_r. The residuals from MLS global fitting contain only noise, which shows that the model describes the experimental data correctly (Figure 3B).

To associate ROA_0 and ROA_r (Figure 3D) with structural elements being present in the polysaccharide scaffold of NA and CA hydrogels, we calculated ROA spectra of trimers of the D-galactose/3,6-anhydro-L-galactopyranose disaccharide and carboxylated derivatives thereof in prototypical conformations (Figure 3C). The NA double α-helix and a single strand α-helix (Figure 4A) were modeled according to the crystal structure of agarose (1AGA).[6b] To obtain representative structures for a carboxylated β-strand we added carboxyl groups to the agarose double α-helix and performed an MD simulation in an explicit water environment. A cluster analysis afforded three conformer families (Figure S4–6): β-strand 'straight', 'bend', and 'reverse bend' (Figure 4B).

We calculated the ROA spectra of ten conformers from the three CA β-strand conformer families and averaged the family member spectra according to their relative weights obtained from the cluster analysis (Figure S6) delivering spectra of the three 'main conformations' being present in CA. The average of the three spectra shows remarkable similarity with ROA_r (Figure 3D) suggesting that the three β-strand motifs are the most important conformational features being present in CA hydrogels and that they are about evenly distributed along the polysaccharide chains. Corresponding bands in ROA_r are for example observed around 1200 cm^{-1} (C1'–O stretch vibration of the glycosidic linkage) or at 1137 and 1086 cm^{-1} (predominantly delocalized C–C stretching vibrations). Interestingly, the single stranded NA α-helix and the average CA β-strand spectrum share a number of characteristic features, while the NA double α-helix spectrum has a considerably different band pattern (Figure 3C). A

negative triplet around 1300 cm^{-1} (mid-chain C–H bending modes) and sharp positive signals at 1204 and 1067 cm^{-1} (C–H bending in all rings and delocalized C–H and O–H bending) are specific for NA double α-helix structure. These features also appear in the ROA_0 spectrum (Figure 3D). The observed spectral differences can be explained by the delocalized C–C stretching modes being locked through the double-helical assembly of the polysaccharide strands, thereby rendering C–H bending modes more dominant. Conversely, the β-strand conformation, where such interlocking is absent, gives rise to strong C–C stretch modes. Hence, the spectral assignments agree with a decrease of double stranded chain organization in favor of β-strand as a response to carboxylation. The same conclusions could be drawn after comparison of experimental and simulated circular intensity differential (CID) spectra (ratio of the above ROA and their parent Raman spectra, Figure S7). As a marked departure from previous studies,[14c-e] it was not necessary to model explicit water interactions with the carbohydrates to obtain an agreement between calculated and observed ROA spectra. This supports the finding that the ROA spectra of NA and CA hydrogels are largely dominated by C–C vibrations being less sensitive to solvent effects.

Considering the proportions obtained from the MLS global fitting, the polysaccharide network in NA hydrogels is built up of ~60% double stranded α-helical and ~40% single stranded domains (Scheme 1A), while in CA β-strand seems to be the predominant conformation (Scheme 1B). This organization as separate chains leaves much weaker interactions resulting in a gel with shear deformable domains.

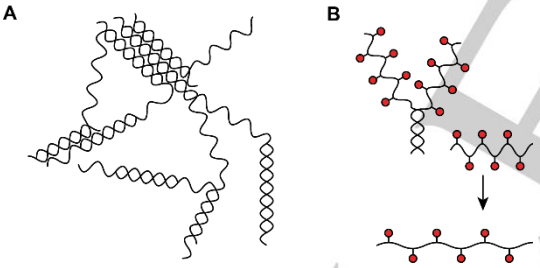

Scheme 1. Networks in agarose-derived hydrogels NA cross-linking depends on the presence of double helices (A). Carboxylation inhibits double helix formation and invokes β-strand secondary structure (B).

In conclusion, the combination of ROA spectroscopy, global fitting and quantum chemical calculations allowed for the elucidation of the secondary structure composition of the polysaccharide agarose and its carboxylated derivative in the gel phase with a particular role for β-strand conformation in the formation of soft physical gels. These insights can be used for the design of tailor-made hydrogels for biomedical and pharmaceutical applications. The field of polysaccharide characterization is of growing importance, for example in the analysis of biopharmaceuticals and their biosimilars, where first studies have employed ROA to elucidate the structure of bioengineered monoclonal antibodies and related molecules with glycosidic appendages.[21] The present study represents a starting point for analyzing polysaccharide higher-order structure in general, similar to, or in combination with, secondary and tertiary structure of proteins and peptides.

Acknowledgements

The authors thank Prof. M. Müller for helpful discussions. This work was supported by the excellence initiative of the German Federal and State Governments Grant EXC 294 (Centre for Biological Signaling Studies) and the University of Freiburg. The Hercules foundation and the Flemish Supercomputing Centre are thanked for generously providing the required CPU resources.

Keywords: Gels • Polysaccharides • Raman Optical Activity • Spectral fitting • Density functional calculations

[1] A. S. Hoffman, *Adv. Drug. Deliver. Rev.* **2012**, *64*, 18–23.
[2] E. Caló, V. V. Khutoryanskiy, *Eur. Polym. J.* **2015**, *65*, 252–267.
[3] T. R. Hoare, D. S. Kohane, *Polymer* **2008**, *49*, 1993–2007.
[4] K. Y. Lee, D. J. Mooney, *Chem. Rev.* **2001**, *101*, 1869–1879.
[5] M. Verhulsel, M. Vignes, S. Descroix, L. Malaquin, D. M. Vignjevic, J. L. Viovy, *Biomaterials* **2014**, *35*, 1816–1832.
[6] a) M. Lahaye, C. Rochas, *Hydrobiologia* **1991**, *221*, 137–148; b) S. Arnott, A. Fulmer, W. E. Scott, I. C. M. Dea, R. Moorhouse, D. A. Rees, *J. Mol. Biol.* **1974**, *90*, 269–284; c) D. A. Rees, E. J. Welsh, *Angew. Chem. Int. Ed.* **1977**, *16*, 214–223.
[7] A. Forget, J. Christensen, S. Lüdeke, E. Kohler, S. Tobias, M. Matloubi, R. Thomann, V. P. Shastri, *Proc. Natl. Acad. Sci. U. S. A.* **2013**, *110*, 12887–12892.
[8] A. Forget, R.-A. Pique, V. Ahmadi, S. Lüdeke, V. P. Shastri, *Macromol. Rapid Commun.* **2015**, *36*, 196–203.
[9] M. Djabourov, A. H. Clark, D. W. Rowlands, S. B. Rossmurphy, *Macromolecules* **1989**, *22*, 180–188.
[10] a) F. J. Zhu, N. W. Isaacs, L. Hecht, G. E. Tranter, L. D. Barron, *Chirality* **2006**, *18*, 103–115; b) L. D. Barron, L. Hecht, E. W. Blanch, A. F. Bell, *Prog. Biophys. Mol. Bio.* **2000**, *73*, 1–49; c) L. D. Barron, *Curr. Opin. Struct. Biol.* **2006**, *16*, 638–643.
[11] a) L. D. Barron, A. R. Gargaro, Z. Q. Wen, *Carbohydr. Res.* **1991**, *210*, 39–49; b) Z. Q. Wen, L. D. Barron, L. Hecht, *J. Am. Chem. Soc.* **1993**, *115*, 285–292.
[12] L. D. Barron, A. D. Buckingham, *Mol. Phys.* **1971**, *20*, 1111–1119.
[13] a) J. Costante, L. Hecht, P. L. Polavarapu, A. Collet, L. D. Barron, *Angew. Chem. Int. Ed.* **1997**, *36*, 885–887; b) K. Ruud, T. Helgaker, P. Bouř, *J. Phys. Chem. A* **2002**, *106*, 7448–7455; c) J. Haesler, I. Schindelholz, E. Riguet, C. G. Bochet, W. Hug, *Nature* **2007**, *446*, 526–529.
[14] a) N. A. Macleod, C. Johannessen, L. Hecht, L. D. Barron, J. P. Simons, *Int. J. Mass Spectrom.* **2006**, *253*, 193–200; b) S. Luber, M. Reiher, *J. Phys. Chem. A* **2009**, *113*, 8268–8277; c) J. R. Cheeseman, M. S. Shaik, P. L. A. Popelier, E. W. Blanch, *J. Am. Chem. Soc.* **2011**, *133*, 4991; d) S. T. Mutter, F. Zielinski, J. R. Cheeseman, C. Johannessen, P. L. A. Popelier, E. W. Blanch, *Phys. Chem. Chem. Phys.* **2015**, *17*, 6016–6027; e) S. T. Mutter, F. Zielinski, C. Johannessen, P. L. A. Popelier, E. W. Blanch, *J. Phys. Chem. A* **2016**, *120*, 1908–1916.
[15] N. R. Yaffe, A. Almond, E. W. Blanch, *J. Am. Chem. Soc.* **2010**, *132*, 10654–10655.
[16] A. F. Bell, L. Hecht, L. D. Barron, *J. Raman Spectrosc.* **1995**, *26*, 1071–1074.
[17] V. Profant, V. Baumruk, X. J. Li, M. Šafařík, P. Bouř, *J. Phys. Chem. B* **2011**, *115*, 15079–15089.
[18] At the given concentration (2% corresponding to ~65 mM in respect to the repetitive disaccharide unit), contributions from primary structure are most likely below the detection limit (compare Ref. 11a: 2–5 M sample concentration for the ROA of monosaccharides).
[19] S. Hirase, *Bull. Chem. Soc. Jpn.* **1957**, *30*, 75–79.
[20] a) R. W. Hendler, R. I. Shrager, *J. Biochem. Bioph. Meth.* **1994**, *28*, 1–33; b) A. Rüther, M. Pfeifer, V. A. Lórenz-Fonfría, S. Lüdeke, *J. Phys. Chem. B* **2014**, *118*, 3941–3949; c) A. Rüther, M. Pfeifer, V. A. Lórenz-Fonfría, S. Lüdeke, *Chirality* **2014**, *26*, 490–496.
[21] a) C. H. Li, T. S. Li, *Curr. Pharm. Biotechno.* **2009**, *10*, 391–399; b) G. Thiagarajan, E. Widjaja, J. H. Heo, J. K. Cheung, B. Wabuyele, X. Mou, M. Shameem, *J. Raman Spectrosc.* **2015**, *46*, 531–536.

Entry for the Table of Contents

Layout 2:

COMMUNICATION

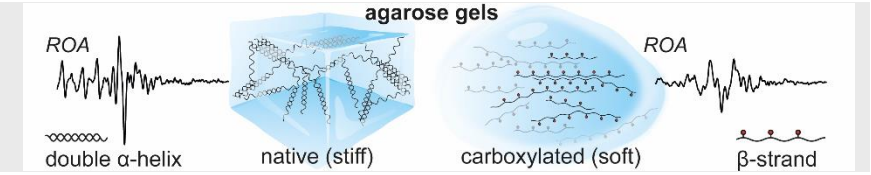

Helix assembly makes the gel stiff: Agarose hydrogels are stiff, but chemical carboxylation of the polysaccharide backbone leads to formation of soft gels. This is because the carboxyl groups prevent inter-chain organization of the polysaccharide as double helices and promotes a β-strand conformation instead. Raman optical activity allows identifying and quantifying such higher order polysaccharide structure directly in the gel phase.

A. Rüther, A. Forget, A. Roy, C. Carballo, F. Mießmer, R. K. Dukor, L. A. Nafie, C. Johannessen, V. P. Shastri, S. Lüdeke**

Page No. – Page No.
Unravelling a direct role for polysaccharide *β*-strands in the higher order structure of physical hydrogels